Available online at www.sciencedirect.com
ScienceDirect
Mendeleev Commun., 2017, **27**, 192–194
Mendeleev Communications

Gas dynamics and kinetics of the penetration of methane–oxygen flames through complex obstacles, as studied by 3D spectroscopy and high-speed cinematography

Nikolai M. Rubtsov,*[a] Alexey N. Vinogradov,[b] Alexander P. Kalinin,[c] Alexey I. Rodionov,[d] Kirill Ya. Troshin,[e] Georgii I. Tsvetkov[a] and Victor I. Chernysh[a]

[a] *Institute of Structural Macrokinetics and Materials Science, Russian Academy of Sciences, 142432 Chernogolovka, Moscow Region, Russian Federation. Fax: +7 495 962 8025; e-mail: nmrubtss@mail.ru*
[b] *Department of Physics, M. V. Lomonosov Moscow State University, 119991 Moscow, Russian Federation*
[c] *A. Yu. Ishlinsky Institute for Problems in Mechanics, Russian Academy of Sciences, 119526 Moscow, Russian Federation*
[d] *Joint Stock Company 'Reagent' Research & Development Center, 125190 Moscow, Russian Federation*
[e] *N. N. Semenov Institute of Chemical Physics, Russian Academy of Sciences, 119991 Moscow, Russian Federation*

DOI: 10.1016/j.mencom.2017.03.029

It was experimentally found that, on the penetration of a flame through obstacles, gas dynamic factors such as flame turbulization can determine the kinetics of combustion, for instance, a transition of low-temperature hydrocarbon combustion to the high-temperature mode.

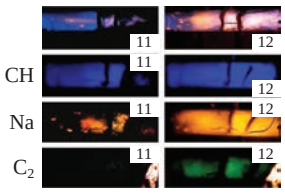

In a breakdown of fire safety, an amount of flammable gas can be released into ambient air. The resulting explosive mixture can endanger the integrity of a vessel, reactor, mine, *etc*. Due to complex branched chain combustion processes and the geometry of a containment, the propagation of a flame front (FF) and the resulting warming-up cannot be simulated with suitable accuracy. The compressible reactive Navier–Stokes equations can be simplified and used for modeling non-isothermal flow only if the flow with a low Mach number is assumed.[1–3] In low speed turbulent combustion applications, the variable-density approximation of low Mach number of the Navier–Stokes equations is an adequate basis for simulation. Nevertheless, any comparison of experimentally recorded FF propagation with the result of numerical modeling is credible only in a qualitative aspect, *e.g.*, on propagation velocity of the boundary of initial and reacting gas, and on the shape of this border. The consideration of detailed kinetics in calculations provides additional uncertainty since most of kinetic parameters are not accurate enough to draw convincing conclusions. The completeness of the kinetic mechanism is reasonably always under question because an important reaction can be overlooked. Moreover, there are no unicity theorems on reactive Navier–Stokes equations; thus, any agreement between calculated and experimental quantities does not argue in favor of the chosen system of equations and the reaction mechanism, as there can be other sets of governing parameters describing the same experimental data.[2,3]

It is known that chemical transformation in blue 'cool' hydrocarbon flames[4,5] is incomplete and some active combustion products can initiate the secondary yellow 'hot'[4] FF propagating over incompletely reacted mixture chemically and thermally activated with a primary blue FF. Note that the color of a blue methane flame is mainly due to CH (431 nm) and CH_2O (470 nm) luminescence, and the yellow color of a flame is caused by the emission of Na atoms excited in 'hot' flame.[4] The reactions of hydrocarbon oxidation to CO occur in a blue flame, and the reactions of CO oxidation to CO_2 occur in a yellow flame. Thus, there is a possibility to share in time these two macrokinetic processes in experiments on flame penetration through obstacles. We have found[6] that the ignition of dilute methane–oxygen mixures (total pressure up to 200 Torr) after a single obstacle with a small circular opening is observed markedly far from an obstacle surface (flame jump). The meshed sphere as an opening leads to an increase in the length of a flame jump through the obstacle, as compared to a round opening.

This work was focused on the comparative contributions of hydrodynamics and chemical kinetics to the penetration of methane–oxygen flames through complex obstacles studied by 3D spectroscopy and color high-speed cinematography.[†]

[†] The experiments were carried out with stoichiometric methane–oxygen mixtures diluted with CO_2 and Kr at initial pressures of 100–200 Torr and 298 K in a horizontal cylindrical quartz reactor 70 cm in length and 14 cm in diameter. The combustible mixture (15.4% CH_4 + 30.8% O_2 + + 46% CO_2 + 7.8% Kr) was prepared; CO_2 was added to decrease FF velocity and to enhance the quality of filming; Kr was added to diminish the discharge threshold. A pair of spark ignition electrodes was located near the butt end of the reactor. The reactor was fixed in two stainless steel gateways at butt-ends, supplied with inlets for gas pumping and blousing and a safety shutter, which swung outward when the total pressure in the reactor exceeded 1 atm.[7] The ignition and flame propagation was observed by an optical 3D spectrometer (hyper spectrometer) and a Casio Exilim F1 Pro color high-speed camera (the frequency of shots was 300–600 s^{-1}). A video file was stored in computer memory and its time-lapse processing was performed.[8–11] The 3D spectrometer[12] simultaneously measured both a horizontal narrow strip on the test object (a spatial coordinate) and a spectral wavelength with a two-dimensional optical detector array. The hyperspectral recording of a combustion process was described elsewhere.[12,13] The speed video filming of combustion and

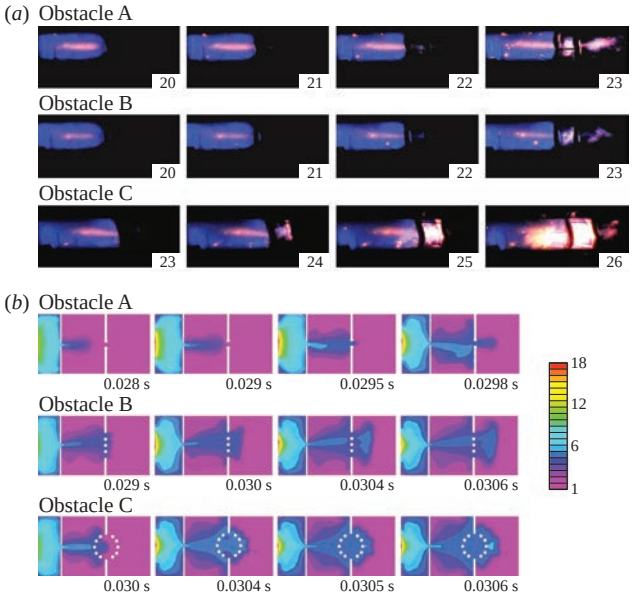

Figure 1 (*a*) High-speed filming and (*b*) results of the numerical modeling of FF propagation through the complex obstacles A, B and C. Gas mixture: 15.4% CH_4 + 30.8% O_2 + 46% CO_2 + 7.8% Kr. Initial pressure, 180 Torr. The figure on each frame corresponds to a frame number after discharge. The scale of dimensionless temperature is presented at the right.

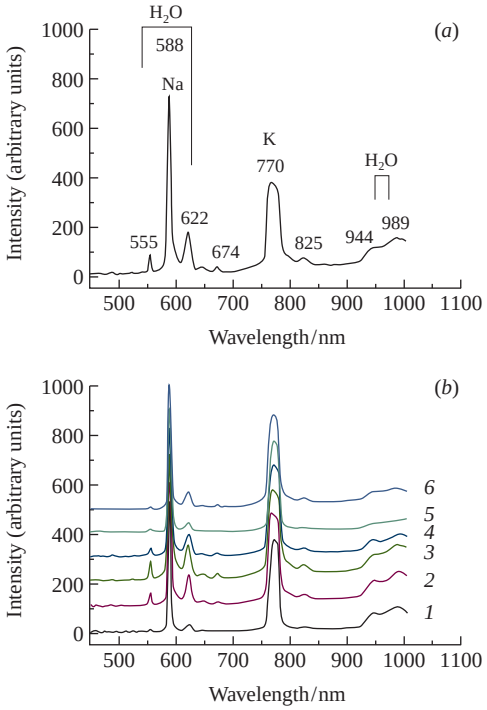

Figure 2 (*a*) Spectrum of the flame at x = 125, y = 30 and (*b*) spectra of the flame along the reactor axis at x = 30, y = (*1*) 1, (*2*) 80, (*3*) 125, (*4*) 160, (*5*) 190 and (*6*) 230 (x is the spatial coordinate, y is the intensity). Gas mixture: 15.4% CH_4 + 30.8% O_2 + 46% CO_2 + 7.8% Kr. Initial pressure, 180 Torr.

The sequences of frames of high-speed filming of FF propagation in a gas mixture through complex obstacles A, B and C are presented in Figure 1.‡ The first center of ignition was observed in close proximity to the surface of the second obstacle for all three obstacles contrary to the case of a single obstacle.[5] It means that the length of a flame jump is mainly determined by gas dynamic factors.

The numerical modeling performed using compressible dimensionless reactive Navier–Stokes equations in low Mach number approximation,[7] which describe flame propagation in a two-dimensional channel,[6,8,12] was qualitatively consistent with experimental data.[6,12]

The problem was solved by finite element analysis using the FlexPDE 6.08 package.[14] Initiation condition was taken as T = 10 on the right boundary of the channel; there was a vertically located orifice in the channel. Boundary conditions (including the orifice) were $C_x = 0$, $C_y = 0$, $n = 0$, $u = 0$, $v = 0$, $\rho_x = 0$, $\rho_y = 0$, and a convective heat exchange $T_t = T - T_0$. A single Arrhenius reaction was considered.

If the second obstacle is placed at the distance of a flame jump after a flat obstacle with a single opening, the first center of ignition is observed in close proximity to the surface of the second obstacle. Such a qualitative difference from flame penetration through a single flat obstacle with the central opening indicates a noticeable role of the interaction of acoustic fluctuations in the reactor containing an obstacle with the propagating front of combustion even for a subsonic flame. Therefore, we took into account the main features of FF propagation through the complex obstacles. In addition, the results obtained by the visualization of FF penetration through orifices of different shape are important for the solution of explosion safety problems for the volumes of complex geometry.

Changes in combustion mechanism at flame penetration through obstacles were investigated by optical spectroscopy. Figure 2 shows the emission spectrum of a diluted methane–oxygen flame and the scanning of the spectra along the reactor axis obtained by 3D spectroscopy. The bands at 600 nm were assigned to water vapor,[12,15] as well as the bands at 944 and 989 nm.[16] The lines at 590 and 770 nm are the hot ones of Na and K atoms, which are usually observed in flame emission.[4] The intensities of spectral bands along a reactor axis change in the same directions because the spectra belong to reaction products or occur in the area of reaction products (Na, K[4]). Thus, the high-temperature mechanism of methane combustion followed by the excitation of alkaline metal bands is realized already after the first obstacle.

To increase the sensitivity of the technique, the change in time of spatial distributions of intermediates characteristic of methane oxidation along with Na line characterizing the value of warming up[4] was monitored with the use of interference filters. These intermediates are CH ($A^1\Delta$–$X^2\Pi$) at 431 nm and C_2 (A^3P_g–X^3P_u) (1–0, 0–0 and 0–1 vibrational transitions) in a range of 470 to 570 nm.[4] The pairs of interference filters of 435 (CH) and 520 nm (C_2) (transition 0–0) and also of 435 and 590 nm (Na) were used to establish the occurrence of intermediates and self-heating as the radiation of Na atoms is caused by thermal excitation at a flame temperature higher than 1200 °C.[4]

Figure 3 shows the results of the high-speed video filming of flame penetration through a flat obstacle 14 cm in diameter with a single opening 25 mm in diameter and the second flat obstacle of the same sizes closed by a flat grid. Only blue luminescence

3D spectrophotometry were carried out simultaneously, or two speed video cameras equipped with interference filters were simultaneously used (Figure S1, see Online Supplementary Materials). The interference filters of 435 nm (40% filter factor, the half-width 15 nm), 520 nm (40% filter factor, the half-width 15 nm) and 590 nm (15% filter factor, the half-width 15 nm) were applied.

‡ Complex obstacles consisted of a flat obstacle 14 cm in diameter with a single opening of 25 mm in diameter (obstacle A), and the second flat obstacle with a single opening 25 mm in diameter (see Figure S1). The second flat obstacle was either a single opening 25 mm in diameter closed with a flat iron net (wire, d = 0.1 mm, cell size of 0.15 mm^2) (obstacle B) or a single opening 40 mm in diameter, into which the net sphere was inserted (obstacle C). The second obstacle was placed at a ~12 cm distance of a flame jump[6] after a flat obstacle with a single opening 25 mm in diameter.

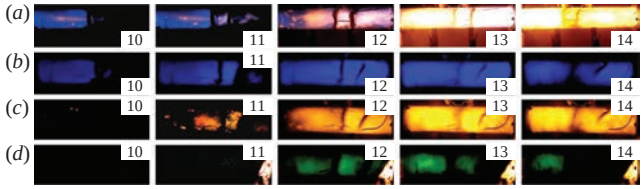

Figure 3 High-speed video filming of penetration of the flame through obstacles A and B: (*a*) no filters and interference filter (*b*) 435 nm, (*c*) 520 nm and (*d*) 590 nm. Gas mixture: 15.4% CH_4 + 30.8% O_2 + 46% CO_2 + 7.8% Kr. Initial pressure, 180 Torr. The figure on each frame corresponds to a frame number after discharge. (*a*), (*d*) Different locations of obstacles after flame penetration are because the frames are obtained for different experiments under the same conditions.

in the reactor caused by the radiation of CH radicals occurred before the first obstacle. The C_2 radicals were detected only after the first obstacle; the greater part of a thermal emission (Na) in the process was observed after the first obstacle, *i.e.*, after turbulization of a reacting gas flow. Thus, the technique used allowed us to separate cold and hot flames in time and space in a single experiment. This result is also important for the verification of numerical models of methane combustion.

Online Supplementary Materials

Supplementary data associated with this article can be found in the online version at doi: 10.1016/j.mencom.2017.03.029.

References

1 O. D. Lopez, R. Moser and O. A. Ezekoye, *Mecánica Comput.*, 2006, **XXV**, 1127.
2 A. Majda, *Equations for Low Mach Number Combustion*, Center of Pure and Applied Mathematics, University of California, Berkeley, 1982, PAM-112.
3 F. Nicoud, *J. Comput. Phys*., 2000, **158**, 71.
4 B. Lewis and G. von Elbe, *Combustion, Flames and Explosions of Gases*, 3rd edn., Academic Press, New York, 1987.
5 I. M. Naboko, N. M. Rubtsov, B. S. Seplyarskii, V. I. Chernysh and G. I. Tsvetkov, *Mendeleev Commun*., 2013, **23**, 163.
6 N. M. Rubtsov, B. S. Seplyarskii, I. M. Naboko, V. I. Chernysh, G. I. Tsvetkov and K.Ya. Troshin, *Mendeleev Commun*., 2015, **25**, 304.
7 N. M. Rubtsov, *The Modes of Gaseous Combustion*, Springer International Publishing, Switzerland, 2016.
8 N. M. Rubtsov, I. M. Naboko, B. S. Seplyarskii, V. I. Chernysh and G. I. Tsvetkov, *Mendeleev Commun*., 2014, **24**, 50.
9 I. M. Naboko, N. M. Rubtsov, B. S. Seplyarskii, K. Ya. Troshin, G. I. Tsvetkov and V. I. Chernysh, *Mendeleev Commun*., 2013, **23**, 358.
10 N. M. Rubtsov, I. M. Naboko, B. S. Seplyarskii, V. I. Chernysh, G. I. Tsvetkov and K. Ya. Troshin, *Mendeleev Commun.*, 2016, **26**, 61.
11 N. M. Rubtsov, A. N. Vinogradov, A. P. Kalinin, A. I. Rodionov, K. Ya. Troshin and G. I. Tsvetkov, *Mendeleev Commun.*, 2015, **25**, 482.
12 N. M. Rubtsov, A. N. Vinogradov, A. P. Kalinin, A. I. Rodionov, I. D. Rodionov, K. Ya. Troshin, G. I. Tsvetkov and V. I. Chernysh, *Fiz.-Khim. Kinet. Gaz. Dinam. (Phys.-Chem. Kinet. Gas Dynam.)*, 2016, **17**, http://chemphys.edu.ru/issues/2016-17-1/articles/597/ (in Russian).
13 N. M. Rubtsov, A. N. Vinogradov, A. P. Kalinin, A. I. Rodionov, I. D. Rodionov, K. Ya. Troshin, G. I. Tsvetkov and V. I. Chernysh, *Fiz.-Khim. Kinet. Gaz. Dinam. (Phys.-Chem. Kinet. Gas Dynam.)*, 2016, **17**, http://chemphys.edu.ru/issues/2016-17-1/articles/615/ (in Russian).
14 G. Backstrom, *Simple Fields of Physics by Finite Element Analysis*, GB Publishing, 2005.
15 T. Icitaga, *Rev. Phys. Chem. Jpn*, 1939, **13**, 96.
16 P.-F. Coheur, P. F. Bernath, M. Carleer, R. Colin, O. L. Polyansky, N. F. Zobov, S. V. Shirin, R. J. Barber and J. Tennyson, *J. Chem. Phys.*, 2005, **122**, 074307.

Received: 16th June 2016; Com. 16/4960